Inorganic Chemistry
Article
Cite This: Inorg. Chem. XXXX, XXX, XXX−XXX
pubs.acs.org/IC

Trivalent Rare-Earth-Metal Bis(trimethylsilyl)amide Halide Complexes by Targeted Oxidations

André M. Bienfait,[†] Benjamin M. Wolf,[‡] Karl W. Törnroos,[†] and Reiner Anwander*[,‡]

[†]Department of Chemistry, University of Bergen, Allégaten 41, N-5007 Bergen, Norway
[‡]Institut für Anorganische Chemie, Universität Tübingen, Auf der Morgenstelle 18, D-72076 Tübingen, Germany

Supporting Information

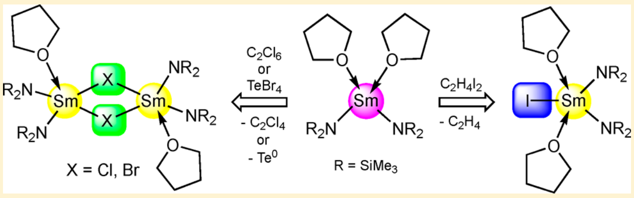

ABSTRACT: In contrast to previously applied salt metathesis protocols the targeted rare-earth-metal compounds Ln[N(SiMe$_3$)$_2$]$_2$(halogenido) were accessed by oxidation of Ln(II) silylamide precursors. Treatment of Sm[N(SiMe$_3$)$_3$]$_2$(thf)$_2$ with 0.5 equiv of C_2Cl_6 or 0.25 equiv of $TeBr_4$ in thf and crystallization thereof gave [Sm{N(SiMe$_3$)$_2$}$_2$(μ-X)(thf)]$_2$ (X = Cl, Br). A similar reaction/crystallization procedure performed with 0.5 equiv of 1,2-diiodoethane gave monomeric Sm[N(SiMe$_3$)$_2$]$_2$I(thf)$_2$. Switching to Yb[N(SiMe$_3$)$_2$]$_2$(thf)$_2$, the aforementioned oxidants generated monomeric five-coordinate complexes Yb[N(SiMe$_3$)$_2$]$_2$X(thf)$_2$ (X = Cl, Br, I). The reaction of Eu[N(SiMe$_3$)$_2$]$_2$(thf)$_2$ with 0.5 equiv of C_2Cl_6 in thf yielded the separated ion pair [Eu{N(SiMe$_3$)$_2$}$_3$Cl][(thf)$_5$Eu(μ-Cl)$_2$Eu(thf)$_5$]. Performing the chlorination in *n*-hexane led to oxidation followed by rapid disproportionation into EuCl$_3$(thf)$_x$ and Eu[N(SiMe$_3$)$_2$]$_3$. The bromination reaction did not afford crystalline material, while the iodination gave crystals of divalent EuI$_2$(thf)$_5$. Use of trityl chloride (Ph$_3$CCl) as the oxidant in thf accomplished the Eu(III) species [Eu{N(SiMe$_3$)$_2$}$_2$(μ-Cl)(thf)]$_2$. In situ oxidation of putative [Tm{N(SiMe$_3$)$_2$}$_2$(thf)$_x$] using 0.5 equiv of C_2Cl_6 in thf followed by crystallization from *n*-hexane led to the formation of a mixture of [Tm{N(SiMe$_3$)$_2$}$_2$(μ-Cl)(thf)]$_2$ and Tm[N(SiMe$_3$)$_2$]$_3$. Switching the oxidant to 0.5 equiv of 1,2-diiodoethane and crystallizing from thf repeatedly afforded the bis-halogenated complex Tm[N(SiMe$_3$)$_2$]I$_2$(thf)$_3$.

INTRODUCTION

Mixed bis(trimethylsilyl)amide halide complexes [Ln{N(SiMe$_3$)$_2$]}$_2$X(thf)$_x$] (Ln = La−Lu, Y, Sc; X = halogenido) represent interesting synthesis precursors, e.g., for organo rare-earth-metal derivatives, as they combine both thermally robust silylamido and halogenido functionalities as easily exchangeable ligands.[1,2] However, their application in organometallic synthesis is impaired by their limited availability originating from (i) hard-to-control LnX$_3$/MNR$_2$ salt metathesis reactions (M = alkali metal), (ii) persistent ate complexation, and (iii) ligand redistribution.[3] The first deliberately obtained example of this class of compounds was reported in 1980, when "ClEu[N(SiMe$_3$)$_2$]$_2$" was assigned as the product (though not isolated) of the reaction of 2 equiv of homoleptic Eu[N(SiMe$_3$)$_2$]$_3$ with 1 equiv of EuCl$_3$ in thf.[4] This in situ formed mixed amide chloride complex was used to reductively generate Eu[N(SiMe$_3$)$_2$]$_2$(thf)$_2$.[5] In 1989, it was reported that the reaction of 2 equiv of Li[N(SiMe$_3$)$_2$] with LnCl$_3$ (Ln = Eu, Gd, Yb, Y) in thf at −5 °C was complete after 30 min.[6] X-ray structure analyses of crystals obtained from *n*-hexane solutions revealed dimeric structures of the composition [Ln{N(SiMe$_3$)$_2$}$_2$(μ-Cl)(thf)]$_2$ (Ln = Gd, Yb). The latter work also included the synthesis and characterization (NMR, microanalysis) of the europium derivative, but the authors pointed out its instability in solution, undergoing disproportionation to Eu[N(SiMe$_3$)$_2$]$_3$ and EuCl$_3$. This disproportionation behavior was found for the yttrium analogue as well: even the crystals, which were proposed as the monomeric bis(thf) adduct Y[N(SiMe$_3$)$_2$]$_2$Cl(thf)$_2$ on the basis of the ^{1}H NMR spectrum, rapidly underwent disproportionation even in the absence of solvent.[6] The authors thought it "most unlikely" that [Ln{N(SiMe$_3$)$_2$}$_2$(μ-Cl)(thf)]$_2$ complexes would exist for rare-earth metals lighter than Sm, since their larger size would lead to a "considerable steric unsaturation and thus instability in solution".[6] However, some 10 years later, the cerium,[7] neodymium,[7] and samarium derivatives[8] were found accessible by both salt metathesis and synproportionation routes. In 2006, inadvertently, the dimeric yttrium species [Y{N(SiMe$_3$)$_2$}$_2$(μ-Cl)(thf)]$_2$ was isolated in an attempt to generate a mixed guanidinate derivative by a one-pot reaction (employing bis(trimethylsilyl)carbodiimide, [(Me$_3$Si)$_2$N]Li(Et$_2$O), and YbCl$_3$ in a 2:2:1 molar ratio).[9] More recently, the dysprosium and praseodymium congeners were obtained via salt metathesis (employing DyCl$_3$ and 2 equiv of Na[N(SiMe$_3$)$_2$] in thf, crystallized from toluene)[10] and a synproportionation approach (employing PrCl$_3$ and 2 equiv of homoleptic Pr[N(SiMe$_3$)$_2$]$_3$ in toluene, crystallized from *n*-hexane/thf), respectively.[11]

Even though the majority of the studied complexes [Ln{N(SiMe$_3$)$_2$}$_2$X(thf)$_x$] feature chlorido ligands, bromido and iodido derivatives are also known. In 1999, [Sm{N(SiMe$_3$)$_2$}$_2$(μ-Br)(thf)]$_2$, was obained by the synproportionation approach (as well as the analogous chloride compound).[8] Two years later,

Received: January 27, 2018

ACS Publications

DOI: 10.1021/acs.inorgchem.8b00240
Inorg. Chem. XXXX, XXX, XXX−XXX

the first iodido derivative [La{N(SiMe$_3$)$_2$}$_2$(μ-I)(thf)]$_2$ was synthesized from LaI$_3$(dme)$_2$ and 2 equiv of K[N(SiMe$_3$)$_2$] in thf, thereafter crystallized from a thf−toluene mixture.[12] Non-ate mixed amide halide complexes bearing other silylamido or alkylamido ligands[13−23] characterized by X-ray structure analysis are shown in Table 1, giving consideration to the amido/halogenido ratio as well as the degree of agglomeration.

Table 1. Non-Ate Mixed Amide Halide (X) Complexes of the Trivalent Rare-Earth Metals

ratio *r* NR$_2$/X	compound	Ln$_x$[a]	ref
2	Nd[N(SiMe$_3$)(C$_6$H$_3$*i*Pr$_2$-2,6)]$_2$Cl(thf)	1	13
	La[N(SiMe$_3$)(C$_6$H$_3$*i*Pr$_2$-2,6)]$_2$Br(thf)	1	14
	Ln(N*i*Pr$_2$)$_2$Cl(thf)$_2$ (Ln = Sc, Lu)	1	15
	[Yb{N(SiMe$_3$)$_2$}$_2$(μ-Cl)]$_2$	2	16
	[Ln{N(SiMe$_3$)$_2$}$_2$(μ-Cl)(thf)]$_2$ (Ln = Ce, Pr, Nd, Sm, Gd, Dy, Y, Yb)	2	6−11, 16
	[Sm{N(SiMe$_3$)$_2$}$_2$(μ-Br)(thf)]$_2$	2	8
	[La{N(SiMe$_3$)$_2$}$_2$(μ-I)(thf)]$_2$	2	12
	[Ln{N(SiHMe$_2$)$_2$}$_2$(μ-Cl)(thf)]$_2$ (Ln = Sc, Y)	2	17
	[Yb{N(SiMe$_3$)(C$_6$H$_3$*i*Pr$_2$-2,6)$_2$}$_2$(μ-Cl)(thf)$_2$]$_2$	2	18
	[Sm(NCy$_2$)$_2$(μ-Cl)(thf)]$_2$[b]	2	19
	[Ln(N*i*Pr$_2$)$_2$(μ-Cl)(thf)]$_2$ (Ln = Sc, Y, La, Lu)	2	15
2 > *r* ≥ 1	Nd$_3$[N(SiHMe$_2$)$_2$]$_5$Cl$_4$(thf)$_2$	4	17
	Sm$_4$(NCy$_2$)$_6$Cl$_6$(thf)$_2$[b]	4	19
	Ce$_5$[N(SiHMe$_2$)$_2$]$_8$Cl$_7$	5	20
0.5	Sc[N(SiMe$_3$)$_2$]Cl$_2$(thf)$_2$	1	21
	Ce[N(SiMe$_3$)$_2$]Br$_2$(thf)$_3$	1	22
	Ln[N(SiMe$_3$)(C$_6$H$_3$*i*Pr$_2$-2,6)]Cl$_2$(thf)$_3$ (Ln = Y, Yb)	1	23
	[Sc(N*i*Pr$_2$)Cl$_2$(thf)]$_4$	4	15

[a] Degree of agglomeration. [b] Cy = cyclohexyl.

As aforesaid, the five-coordinate monomeric species Y[N(SiMe$_3$)$_2$]$_2$Cl(thf)$_2$ was postulated on the basis of NMR studies, but a structural proof was not provided. Herein, we present the syntheses and X-ray structure analyses of monomeric mixed halide bis(trimethylsilyl)amide rare-earth-metal complexes of the type Ln[N(SiMe$_3$)$_2$]$_2$X(thf)$_2$ (Ln = Yb, X = Cl, Br, I; Ln = Sm, X = I).

■ RESULTS AND DISCUSSION

Precursor Selection. All complexes under study were accessed through redox protocols employing divalent silylamides Ln[N(SiMe$_3$)$_2$]$_2$(thf)$_2$ (Ln = Sm, Eu, Yb) and commercially available oxidants. In the course of this study, the solid-state structures of Ln[N(SiMe$_3$)$_2$]$_2$(thf)$_2$ (Ln = Eu, Yb) were determined. Even though the compounds have been routinely used as precursors for several decades, to the best of our knowledge X-ray structure analyses have not yet been published. The molecular structures and geometrical parameters are given in Figures S1 and S2 in the Supporting Information and are similar to those of the known Sm[N(SiMe$_3$)$_2$]$_2$(thf)$_2$,[24] Eu[N(SiMe$_3$)$_2$]$_2$(dme)$_2$,[5] and Yb[N(SiMe$_3$)$_2$]$_2$(dmpe)$_2$ (dmpe = 1,2-bis(dimethylphosphino)ethane).[25] The oxidants employed have all proven their usefulness in organolanthanide chemistry already. Hexachloroethane, 1,2-diibromoethane, and 1,2-diiodoethane were employed, for example, to oxidize divalent ytterbium and samarium aryloxides to trivalent bis(aryloxide) halide complexes.[26,27] Tellurium tetrabromide was applied to oxidize Ce[N(SiMe$_3$)$_2$]$_3$, yielding Ce[N(SiMe$_3$)$_2$]$_3$Br,[22,28] with moderate success, however. 1,2-Diiodoethane was also the reagent of choice to generate Cp*$_2$SmI(thf) from Cp*$_2$Sm(thf)$_2$.[26b,29] Trityl chloride showed its potential in Ce(III) to Ce(IV) oxidations, giving high-yield access to tetravalent heteroleptic and homoleptic silylamide complexes Ce[N(SiMe$_3$)$_2$]$_3$Cl[30] and Ce[N(SiHMe$_2$)$_2$]$_4$,[20] respectively. The byproducts occurring in these redox protocols are easily separable as (a) a volatile liquid (tetrachloroethene in the chlorination), (b) elemental metal (tellurium in the bromination), or (c) a gas (ethylene in the iodination and bromination). Therefore, especially the use of 1,2-diiodoethane and 1,2-dibromoethane as oxidation reagents comes in handy for producing the halogenated species as an intermediate in consecutive one-pot reactions.

Samarium and Ytterbium Derivatives. All four oxidation protocols employing Ln[N(SiMe$_3$)$_2$]$_2$(thf)$_2$ (Ln = Sm, Yb) and either 0.5 equiv of C$_2$Cl$_6$, 0.25 equiv of TeBr$_4$, 0.5 equiv of BrCH$_2$CH$_2$Br or 0.5 equiv of ICH$_2$CH$_2$I in thf and yielding [Ln{N(SiMe$_3$)$_2$}$_2$(μ-X)(thf)]$_2$ (Ln = Sm, X = Cl (**1**), Br (**2**)) and Ln[N(SiMe$_3$)$_2$]$_2$X(thf)$_2$ (Ln = Sm, X = I (**3**); Ln = Yb, X = Cl (**4**), Br (**5**), I (**6**)) proved to be simple, viable, and highly efficient routes.

The samarium chlorination and bromination products, [Sm{N(SiMe$_3$)$_2$]}$_2$(μ-X)(thf)]$_2$ (X = Cl (**1**), Br (**2**)) were crystallized from thf and revealed the same μ_2-bridging arrangement as found previously, when the complexes were crystallized from *n*-pentane (Scheme 1).[8] Crystallization at 7 °C from *n*-pentane[31] and crystallographic analyses at 223 K implied space groups $P2_1/n$ (**1**) and *Pbca* (**2**),[8] while in this work, **1** and **2** were crystallized at −40 °C from thf and crystallographically studied at 123 K, in space groups $C2/c$ and $P\bar{1}$, respectively (Figures S3 and S4).

Scheme 1. Halogenation of Ln[N(SiMe$_3$)$_2$]$_2$(thf)$_2$ (Ln = Sm, Yb) Resulting in the Known Dimeric Structures [Sm{N(SiMe$_3$)$_2$}$_2$(μ-X)(thf)]$_2$ (X = Cl (1), Br (2)) and Monomeric Five-Coordinate Ln[N(SiMe$_3$)$_2$]$_2$X(thf)$_2$ (Ln = Sm, X = I (3); Ln = Yb, X = Cl (4), X = Br (5), X = I (6))[a]

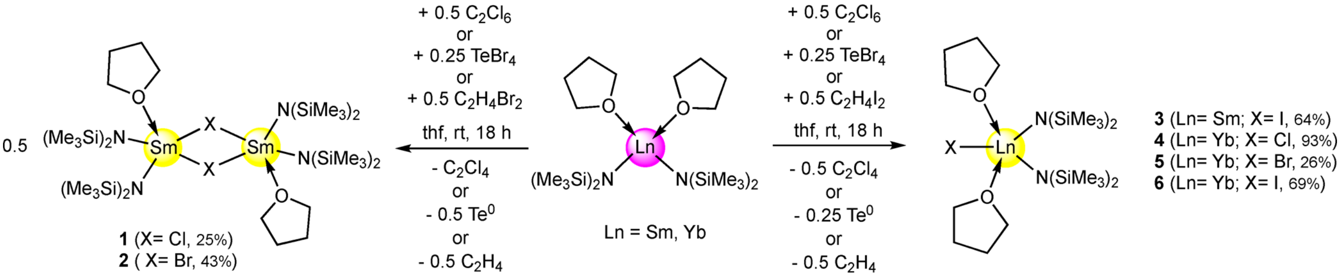

[a] Crude yields are a minimum of 85% for all reactions. Crystallized yields are given.

DOI: 10.1021/acs.inorgchem.8b00240
Inorg. Chem. XXXX, XXX, XXX−XXX

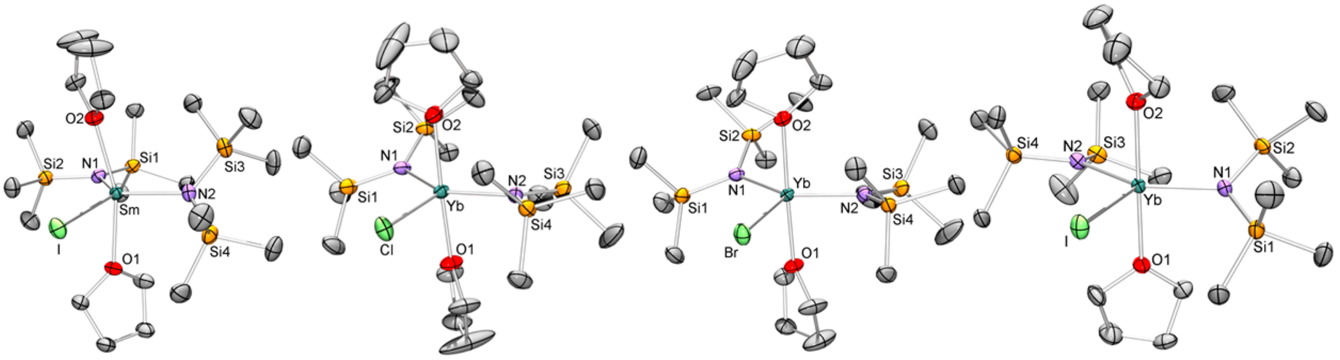

Figure 1. Crystal structures of Ln$[N(SiMe_3)_2]_2X(thf)_2$ (from left to right: **3** (Ln = Sm, X = I), **4** (Ln = Yb, X = Cl), **5** (Ln = Yb, X = Br), and **6** (Ln = Yb, X = I)). Hydrogen atoms are omitted for clarity. Atoms are represented by atomic displacement ellipsoids at the 50% level. For selected interatomic distances and angles, see Table 2.

The iodination of Sm$[N(SiMe_3)_2]_2(thf)_2$, on the other hand, led to monomeric Sm$[N(SiMe_3)_2]_2I(thf)_2$ (**3**) (Scheme 1), with the metal center coordinated in a distorted-trigonal-bipyramidal fashion (Figure 1 and Table 2). Nitrogen atoms N1 and N2, together with the iodine, span the trigonal plane, whereas O1 and O2 represent the apical positions. A similar arrangement was found in the aryloxide complex Sm$(OC_6H_2tBu_2\text{-}2,6\text{-}Me\text{-}4)_2I(thf)_2$.[31] The Sm−I bond in **3** is slightly longer than in the aryloxide complex (3.1011(2) vs 3.024(2) Å), while the Sm−O(thf) distances are practically identical (2.4213(13) and 2.4299(13) vs 2.424(7) Å). The Sm−N bonds are comparable (on average slightly shorter) to those in the five-coordinate complex Sm$[N(SiHMe_2)_2]_3(thf)_2$ (2.3099(15) and 2.2853(15) vs 2.302(3)−2.330(3) Å).[32] The ^{1}H NMR spectra of compounds **1**−**3** recorded in $[D_8]$thf at ambient temperature revealed only one signal for the $SiMe_3$ groups at −0.12 ppm (**1**), −0.19 ppm (**2**), and −0.31 ppm (**3**). For dimeric complexes **1** and **2**, an additional $SiMe_3$ resonance appeared in C_6D_6, assignable to homoleptic Sm$[N(SiMe_3)_2]_3$ (see the Supporting Information). This behavior was not found for monomeric complex **3** and is likely due to ligand redistribution processes occurring in non-coordinating solvents such as C_6D_6.

Table 2. Selected Bond Lengths (Å) and Angles (deg) for Complexes Ln$[N(SiMe_3)_2]_2X(thf)_2$ (3−6)

	3[a] (Sm/I)	**4**[b] (Yb/Cl)	**5**[b] (Yb/Br)	**6**[b] (Yb/I)
Ln−X	3.1011(2)	2.503(1)	2.6713(3)	2.9017(2)
Ln−N1	2.310(2)	2.231(4)	2.235(2)	2.235(2)
Ln−N2	2.285(2)	2.221(4)	2.227(2)	2.228(2)
Ln−O1	2.421(1)	2.313(3)	2.312(2)	2.309(2)
Ln−O2	2.430(1)	2.319(4)	2.316(2)	2.305(2)
Ln−N1−Si1	126.72(8)	122.5(2)	122.6(1)	122.8(1)
Ln−N1−Si2	113.27(8)	119.5(2)	119.4(1)	119.6(1)
Ln−N2−Si3	121.72(8)	119.0(2)	117.3(1)	114.9(1)
Ln−N2−Si4	121.26(8)	121.7(2)	122.9(1)	124.9(1)
N1−Ln−N2	124.16(5)	144.5(2)	145.37(8)	146.47(8)
N1−Ln−X	133.63(4)	110.8(1)	110.61(6)	109.64(6)
N2−Ln−X	102.15(4)	104.8(1)	103.92(6)	103.68(6)
O1−Ln−O2	162.68(5)	177.6(1)	177.39(8)	178.71(7)
O1−Ln−X	86.19(3)	91.5(1)	91.99(5)	91.80(5)
O2−Ln−X	84.12(3)	90.9(1)	90.58(5)	89.49(5)

[a]Monoclinic $P2_1/n$. [b]Orthorhombic $P2_12_12_1$.

For ytterbium, all oxidation products (**4**−**6**) crystallized from thf in the five-coordinate, monomeric fashion as for samarium compound **3** (Scheme 1, Figure 1, and Table 2). Chloride and iodide complexes **4** and **6** are again comparable with their aryloxo counterparts Yb$(OC_6H_2tBu_2\text{-}2,6\text{-}Me\text{-}4)_2X(thf)_2$ (X = Cl,[33] I[26b]). In **4**, the Yb−Cl bond is slightly longer than in the respective aryloxide (2.503(1) vs 2.477(9) Å), with very similar Yb−O(thf) distances (2.313(3) and 2.319(4) vs 2.295(1) Å). In contrast, the Yb−I bond in **6** appears slightly shorter (2.9017(2) vs 2.916(2) Å), with Yb−O(thf) distances being basically the same (2.309(2) and 2.305(2) vs 2.304(6) Å). The Yb−N bonds are by nature significantly longer than the Yb−O(Ar) bonds (2.2349(15) and 2.2284(16) vs 2.071(5) Å). The average Yb−N bond lengths of 2.231(2) Å (**4**) and 2.232(2) Å (**6**) are comparable to that in six-coordinate Yb$[N(SiMe_3)(C_6H_3iPr_2\text{-}2,6)]Cl_2(thf)_3$ (2.218(5) Å).[18] The silylamido ligands in samarium complex **3** and ytterbium complexes **4**−**6** seem not to engage in any significant agostic distortions, as evidenced by similar Ln−N−Si angles (114.9(1)−124.9(1)°) and Ln- - -Si distances larger than 3.33 Å.

For comparison, the reaction of $YbCl_3$ with 2 equiv of Li$[N(SiMe_3)_2]$ in thf, followed by vacuum treatment at ca. 50 °C and crystallization from toluene, gave single-crystalline $[Yb\{N(SiMe_3)_2\}_2(\mu\text{-}Cl)(thf)]_2$. Formation of the chlorido-bridged dimer is most likely due to a shortage of thf in the final crystallizing mixture, although one can speculate about the implications of different precursors for final product aggregation. Our redox approach involves a preset $[Ln\{N(SiMe_3)_2\}_2]$ arrangement, while the stepwise introduction of silylamido ligands along the salt metathesis route might favor the formation of chlorido-bridged species.

On examination of the effect of increasing halogen size on the coordination geometry of complexes **4**−**6**, a clear trend appears. The increasing halogen size from X = Cl to X = I caused the X−Yb−N1,2 angles to decrease about 1° each (Table 2). Accordingly, the N1−Yb−N2 angle increases about 2° from complex **4** to complex **6** (Table 2). Furthermore, it appears that amido ligand N1 is not affected by the halogen size and remains fairly symmetric, as can be seen by the Yb−N1−Si1,2 angles, which deviate by only about 3° (Table 2). On the other hand, an increasing halogen size seems to have an effect on the amido ligand N2, as reflected by steadily decreasing Yb−N2−Si3 angles and increasing Yb−N2−Si3 angles. In compound **4** the angles Yb−N2−Si3 and Yb−N2−Si4 differ less than 3°. This discrepancy grows to 10° in compound **6**. Other parameters, such as O−Yb−O and O−Yb−X angles, do not seem to underlie specific size-dependent trends.

Europium Derivatives. Once more, europium revealed a (redox) reaction behavior distinct from ytterbium and samarium,

DOI: 10.1021/acs.inorgchem.8b00240

Scheme 2. Synthesis of Ion-Pair Compound 7 and Oxidation of $Eu[N(SiMe_3)_2]_2(thf)_2$ with Trityl Chloride in THF Yielding $[Eu\{N(SiMe_3)_2\}_2(\mu\text{-}Cl)(thf)]_2$ (8)[a]

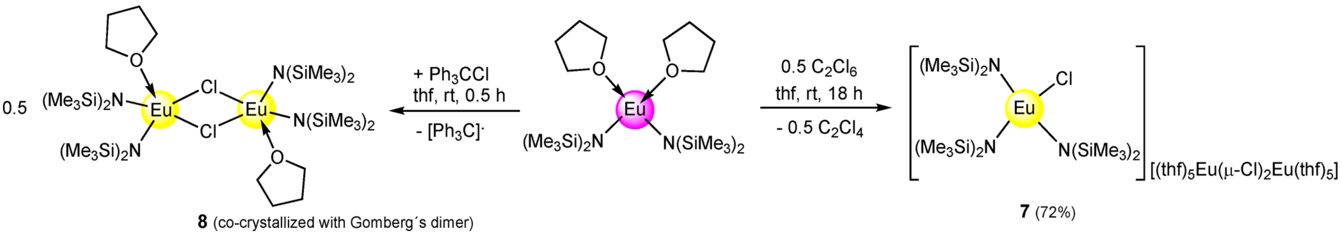

[a] Crystallized products/yields are shown.

albeit employing identical oxidation protocols.[34] An initial attempt to chlorinate $Eu[N(SiMe_3)_2]_2(thf)_2$ with 0.5 equiv of C_2Cl_6 in *n*-hexane (instead of THF) led to an oxidation followed by an instant disproportionation to homoleptic $Eu[N(SiMe_3)_2]_3$ and $EuCl_3(thf)_x$, as described earlier.[6] If the reaction was conducted in thf, such a disproportionation behavior was not observed (Scheme 2). A concentrated thf solution of the crude product was kept at −40 °C for approximately 4 weeks until crystals formed.

Instead of finding the trivalent mixed silylamide chloride compound $[Eu\{N(SiMe_3)_2\}_2(\mu\text{-}Cl)(thf)]_2$ analogous to Sm, we identified the incompletely oxidized trimetallic complex $[Eu\{N(SiMe_3)_2\}_3Cl][(thf)_5Eu(\mu\text{-}Cl)_2Eu(thf)_5]$ (7) by X-ray structure analysis (Figure 2). Complex **7** features an ion-pair structure with the four-coordinate anionic unit $[Eu\{N(SiMe_3)_2\}_3Cl]$ and the μ_2-chloro-bridged Eu_2 cationic moiety $[(thf)_5Eu(\mu\text{-}Cl)_2Eu(thf)_5]$. The overall composition of the anionic unit $[Eu\{N(SiMe_3)_2\}_3Cl]$ is comparable to that found in trivalent ate complexes $[Ln\{N(SiMe_3)_2\}_3Cl]^-[Li(thf)_4]^+$ (Ln = Sm,[35] Y[36]) or the tetravalent cerium complex $Ce[N(SiMe_3)_2]_3Cl$.[37] By comparison of the Eu−X metrical parameters in **7** (Eu−N, average 2.308 Å; Eu−Cl, 2.619(1) Å) with those reported for $[Sm\{N(SiMe_3)_2\}_3Cl]^-[Li(thf)_4]^+$ (Sm−N, average 2.321 Å; Ln−Cl, 2.631(2) Å)[35] and $[Y\{N(SiMe_3)_2\}_3Cl]^-[Li(thf)_4]^+$ (Y−N, average 2.25 Å; Y−Cl, 2.55 Å)[36] the composition of **7** is best described as a monoanion/monocation pair. Accordingly, this renders the disordered and symmetry-related entity $[(thf)_5Eu(\mu\text{-}Cl)_2Eu(thf)_5]$ monocationic, formally (and favorably) involving Eu(III) and Eu(0) centers (unlikely alternative: Eu(II) and Eu(I)). It is noteworthy that a dicationic unit has been detected previously in $[(thf)_4Yb(\mu\text{-}Cl)_2Yb(thf)_4]^{2+}[Ph_3C]^-{}_2$,[38] with the exception that the smaller Yb^{2+} ions are coordinated by four thf molecules. As in complexes **1**−**6**, the amido ligands in **7** do not exhibit any significant secondary intramolecular interactions.

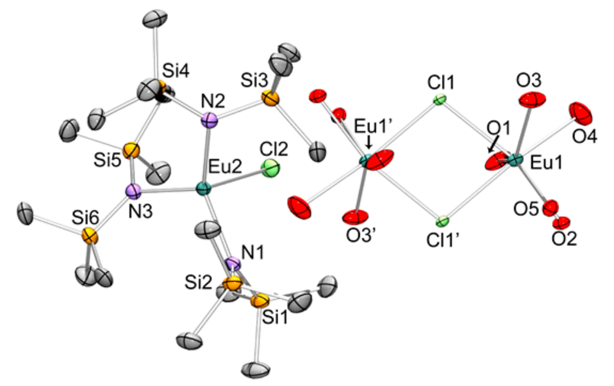

Figure 2. Crystal structure of complex **7**. Hydrogen and thf carbon atoms are omitted for clarity. Atoms are represented by atomic displacement ellipsoids at the 40% level. Cl1 is disordered over two positions. Only the major position is visualized. Selected interatomic distances (Å) and angles (deg) (symmetry transformations used to generate equivalent atoms: (′) −*x* + 1, −*y* + 2, −*z* + 1): Eu1−Cl1 2.886(11), Eu1−Cl1′ 2.8523(14), Eu1−O_{thf} 2.540(4)−2.638(3), Eu2−N1 2.302(4), Eu2−N2 2.304(3), Eu2−N3 2.317(4), Eu2−Cl2 2.6188(11), Eu1···Eu1′ 4.4080(4), Eu···Si > 3.4166(13); N1−Eu2−N2 115.33(13), N2−Eu2−N3 115.86(12), N3−Eu2−N1 116.59(13), N1−Eu2−Cl2 101.17(9), N2−Eu2−Cl2 101.97(9), N3−Eu2−Cl2 102.28(9), Cl1−Eu1−Cl1′ 79.69(4), Eu1−Cl1−Eu1′ 100.32(4), Eu2−N1−Si1 115.44(19), Eu2−N1−Si2 124.62(19), Eu2−N2−Si3 115.66(18), Eu2−N2−Si4 123.03(19), Eu2−N3−Si5 116.25(18), Eu2−N3−Si6 121.2(2), Si1−N1−Si2 119.7(2), Si3−N2−Si4 121.1(2), Si5−N3−Si6 122.4(2).

Iodination of $Eu[N(SiMe_3)_2]_2(thf)_2$ with 0.5 equiv of ICH_2CH_2I in thf led, upon storage at −40 °C, after a few weeks to the crystallization of $EuI_2(thf)_5$.[39] Unfortunately, we did not succeed in the isolation of any crystalline bromination product via application of $TeBr_4$.

Use of the more powerful oxidant trityl chloride in an equimolar reaction with $Eu[N(SiMe_3)_2]_2(thf)_2$ in thf finally gave the desired trivalent product $[Eu\{N(SiMe_3)_2\}_2(\mu\text{-}Cl)(thf)]_2$ (**8**) (Scheme 2, Figure 3, and Table 3). Crystals of **8** were harvested from a concentrated thf solution as orange irregular chunks and not in dark red prisms, as reported from *n*-pentane.[6] As a crystallographic remark, complex **8** is the only compound of this family known so far which includes 1.5 molecules of the dimer and 2 molecules of lattice solvent (thf) in the asymmetric unit (Figure S5). The isolation and characterization of **8** are

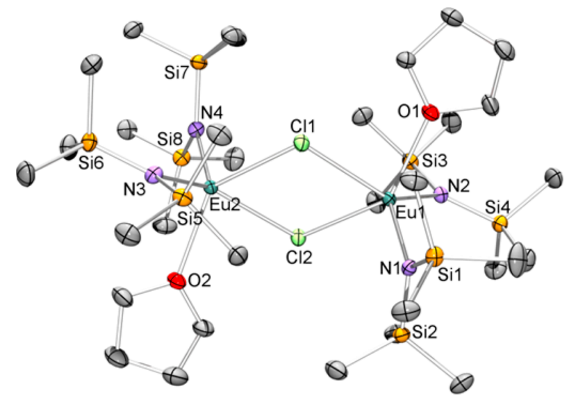

Figure 3. Crystal structure of molecule A (out of 1.5 in the asymmetric unit) of $[Eu\{N(SiMe_3)_2\}_2(\mu\text{-}Cl)(thf)]_2$ (**8**; cf. Figure S5). Hydrogen atoms and lattice solvent (two molecules of thf) are omitted for clarity. Atoms are represented by atomic displacement ellipsoids at the 50% level. Selected interatomic distances and angles are given in Table 3.

DOI: 10.1021/acs.inorgchem.8b00240
Inorg. Chem. XXXX, XXX, XXX−XXX

Table 3. Selected Bond Lengths (Å) and Angles (deg) of Dimeric Complexes [Ln{N(SiMe$_3$)$_2$}$_2$(μ-X)(thf)]$_2$ (1, 2, 8, 9)

	1	2	8[a]	9
Ln1−X1	2.821(1)	2.9553(2)	2.7842(8)	2.6902(3)
Ln1−X2(′)	2.758(1)	2.9656(2)		2.6916(3)
Ln1−N1	2.297 (4)	2.251(1)	2.249(3)	2.182(2)
Ln1−N2	2.254(5)	2.272(1)	2.277(3)	2.205(2)
Ln1−O1	2.453(5)	2.461(1)	2.454(2)	2.357(1)
X−Ln1−X	74.90(5)	76.037(5)	73.52(2)	75.02(1)
N1−Ln1−N2	114.8(2)	120.21(5)	113.79(9)	115.44(5)
X2(′)−Ln1−O1	75.71(11)	79.22(3)	79.14(6)	79.24(3)
Ln−X−Ln	105.10(5)	103.963(5)	106.41(2)	104.98(1)

[a] Average from two molecules.

hampered by the formation of Gomberg's dimer, the trityl radical coupling coproduct. To investigate the extent of conversion, the reaction was repeated in the presence of 1 equiv of hexamethylbenzene (C_6Me_6). The reaction mixture was dried under vacuum, and integration of the characteristic ^{1}H NMR spectroscopic signals of Gomberg's dimer against C_6Me_6 proved quantitative conversion (Figure S8).

Overall, the formation of oxidized monomeric and dimeric mixed bis(trimethylsilyl)amide halide complexes Ln[N(SiMe$_3$)$_2$]$_2$X(thf)$_2$ and [Ln{N(SiMe$_3$)$_2$}$_2$(μ-X)(thf)]$_2$, respectively, in thf solutions is clearly dependent on the redox potential and size of the metal as well as the size of the halogenido anion X. A similar size dependence was found in the selective oxidation of divalent samarium aryloxides with I_2 and 1,2-dichloroethane or *t*BuCl, respectively.[27]

Thulium Derivatives. Spurred by the applicability of such redox protocols for the "classical" divalent lanthanides (Eu(II), Sm(II), Yb(II)), we turned our attention to thulium(II). Due to its extremely reducing character, putative "Tm[N(SiMe$_3$)$_2$]$_2$(thf)$_x$" has not yet been isolated.[40] Therefore, the oxidation reactions had to be conducted in situ and at low temperatures (−40 °C). The reaction of TmI$_2$(thf)$_3$ with 2 equiv of Na[N(SiMe$_3$)$_2$] in thf at −40 °C, followed by the addition of 0.5 equiv of C_2Cl_6, led after workup to the isolation of [Tm{N(SiMe$_3$)$_2$}$_2$(μ-Cl)(thf)]$_2$ (**9**) from an *n*-hexane solution (Scheme 3).

The heteroleptic complex was "contaminated" with cocrystallizing homoleptic Tm[N(SiMe$_3$)$_2$]$_3$, which might have formed by ligand redistribution of heteroleptic complex **9** in the aliphatic solvent or by a redox disproportionation from "Tm[N(SiMe$_3$)$_2$]$_2$(thf)$_x$" with elemental Tm as a coproduct. For this reaction setup, the use of *n*-hexane in the workup was required, since sodium iodide displays a high solubility in thf. X-ray diffraction data including molecular drawings and metrical parameters of **9** (Figure S6; cf. Table 3) and Tm[N(SiMe$_3$)$_2$]$_3$ (Figure S7) have been placed in the Supporting Information.

Scheme 3. Halogenation of Putative "Tm[N(SiMe$_3$)$_2$]$_2$(thf)$_x$" Obtained in Situ from TmI$_2$(thf)$_3$ and M[N(SiMe$_3$)$_2$] (M = Na, K), Resulting in [Tm{N(SiMe$_3$)$_2$}$_2$(μ-Cl)(thf)]$_2$ (9) and Monomeric Six-Coordinate Tm[N(SiMe$_3$)$_2$]I$_2$(thf)$_3$ (10)

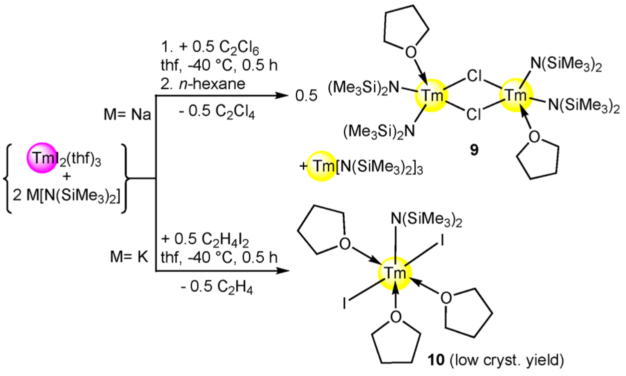

Addition of 0.5 equiv of $C_2H_4I_2$ to "Tm[N(SiMe$_3$)$_2$]$_2$(thf)$_x$", formed in situ from TmI$_2$(thf)$_3$ and 2 equiv of K[N(SiMe$_3$)$_2$], led to the isolation of the bis-halogenated product Tm[N(SiMe$_3$)$_2$]I$_2$(thf)$_3$ (**10**) (Scheme 3 and Figure 4). Analogous reactions with C_2Cl_6 and TeBr$_4$ as oxidants gave crystals that decomposed within seconds after being taken out of the mother liquor, ruling out any crystallographic analysis. Although **10** is a rare example of a discrete mono(amido) bis(halogenido) Ln(III) derivative, the oxidation route via the "non-classical" divalent Tm(II) species seems too elaborate. Complex **10** features a pseudo-octahedral coordination sphere, with the bis(trimethylsilyl)amido ligand and one thf molecule (O3) in the apical positions, while the three thf molecules build up a *mer* configuration. The closest analogues seem to be Ln[N(SiMe$_3$)(C$_6$H$_3$*i*Pr$_2$-2,6)]Cl$_2$(thf)$_3$ (Ln = Y, Yb),[18] Sc[N(SiMe$_3$)$_2$]Cl$_2$(thf)$_2$,[21] and Ce[N(SiMe$_3$)$_2$]Br$_2$(thf)$_3$ (cf. Table 1).[22] The Tm−N bond length in **10** (2.196(4) Å) is in

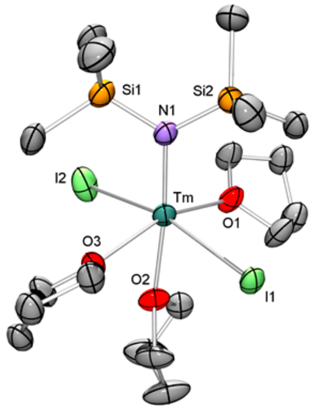

Figure 4. Crystal structure of Tm[N(SiMe$_3$)$_2$]I$_2$(thf)$_3$ (**10**). Hydrogen atoms and lattice solvent (one molecule of thf) are omitted for clarity, as is the second disorder component of thf (O2). Atoms are represented by atomic displacement ellipsoids at the 50% level. Selected interatomic distances (Å) and angles (deg): Tm−N1 2.196(4), Tm−I1 3.0074(4), Tm−I2 2.9893(4), Tm−O1 2.291(4), Tm−O2 2.44(2), Tm−O3 2.304(3), Tm···Si1 3.442(2), Tm···Si2 3.457(2); I1−Tm−I2 164.290(17), N1−Tm−O3 100.44(15), O1−Tm−O3 158.12(14), N1−Tm−I1 97.08(10), N1−Tm−I2 98.63(10), N1−Tm−O1 101.41(15), N1−Tm−O2 174.8(3), Tm−N1−Si1 121.9(2), Tm−N1−Si2 122.7(2), Si1−N1−Si2 115.4(3).

agreement with those observed in Ln[N(SiMe$_3$)(C$_6$H$_3$*i*Pr$_2$-2,6)]Cl$_2$(thf)$_3$ (Ln = Y (**A**), Yb (**B**)) (2.260(2), 2.218(5) Å), Sc[N(SiMe$_3$)$_2$]Cl$_2$(thf)$_2$ (**C**) (2.039(2) Å), and Ce[N(SiMe$_3$)$_2$]Br$_2$(thf)$_3$ (**D**) (2.331(3) Å). The *trans*-positioned iodido ligands in **10** display similar Tm−I distances of 3.0074(4) and 2.9893(4) Å, in accordance with the Y−Cl (2.54945(5), 2.5793(5) Å), Yb−Cl (2.550(2), 2.544(2) Å), and Sc−Cl distances (2.379(1), 2.398(1) Å) in **A**−**C**, respectively.

It is noteworthy that in **D** the Ce−Br bond lengths differ from each other due to their asymmetric arrangement in the molecule (2.9115(5) vs 2.8854(5) Å). The two thf molecules in **10** occupying the residual *trans* positions in the equatorial plane show similar Tm−O bond lengths (2.291(4), 2.304(3) Å), which however are significantly shorter than the Tm−O(apical) distance of 2.44(2) Å. The same situation was detected in **B** with Yb−O bond lengths (2.300(5), 2.325(5) vs 2.439(5) Å) being almost identical with those of **10**. The apical-positioned ligands are in nearly perfect alignment with the central atom, as seen from the N1−Tm−O3 angle of 174.8(3)°. The bulky silylamido ligand seemingly pushes the equatorial ligands toward the apical thf, as indicated by angles N1−Tm−I (97.08(1) and 98.63(10)°) and N1−Tm−O(equatorial) (101.41(15) and 101.33(15)°).

■ CONCLUSIONS

The oxidative routes applied for the synthesis of rare-earth-metal bis(trimethylsilyl)amide halide complexes of the type [Ln{N(SiMe$_3$)$_2$}$_2$X(thf)$_x$] using the divalent precursors Ln[N(SiMe$_3$)$_2$]$_2$(thf)$_2$ (Ln = Sm, Yb) proved to be simple, easily applicable, and highly efficient. Facile separation of byproducts (volatiles or elemental metal formation originating from the use of C$_2$Cl$_6$, C$_2$H$_4$I$_2$, C$_2$H$_4$Br$_2$, and TeBr$_4$) comes in particularly handy and might allow consecutive one-pot reactions with halogenated intermediate species (e.g., use of 1,2-diiodoethane). The mononuclear trivalent species [Ln{N(SiMe$_3$)$_2$}$_2$X(thf)$_x$] are obtained for smaller Ln(III) (Yb) independent of the size of X, while for a larger Ln(III) such as Sm(III) only the large iodide ligands allowed for the isolation of a monometallic species. The well-known dimeric [Ln{N(SiMe$_3$)$_2$}$_2$(μ-X)(thf)]$_2$ are formed in the presence of smaller X, as shown for the combinations Sm/Cl, Sm/Br, and Eu/Cl. In the europium case the strength of the oxidant plays an important role, as shown for the isolation of trivalent [Eu{N(SiMe$_3$)$_2$}$_2$(μ-Cl)(thf)]$_2$ using trityl chloride and the unusual incompletely oxidized [Eu{N(SiMe$_3$)$_2$}$_3$Cl][(thf)$_5$Eu(μ-Cl)$_2$Eu(thf)$_5$] from treatment of Eu[N(SiMe$_3$)$_2$]$_2$(thf)$_2$ with 0.5 equiv of C$_2$Cl$_6$. Performing this chlorination on the elusive, "non-classical" divalent precursor [Tm{N(SiMe$_3$)$_2$}$_2$(thf)$_x$] gave access to the monohalogenated species [Tm{N(SiMe$_3$)$_2$}$_2$(μ-Cl)(thf)]$_2$ but was less straightforward than the samarium and ytterbium reactions because of product contamination with cocrystallized homoleptic Tm[N(SiMe$_3$)$_2$]$_3$. The 1,2-diiodoethane-promoted iodination reaction also took a different pathway, generating the mono[bis(trimethylsilyl)amide] bis(halide) complex Tm[N(SiMe$_3$)$_2$]I$_2$(thf)$_3$.

Finally, the present study not only embarks on an alternative strategy for the synthesis of rare-earth-metal compounds of the type "Ln[N(SiMe$_3$)$_2$]$_x$(halogenido)$_y$" ($x + y = 3$) but might be also enlightening from the perspective of organic chemistry. In particular, Evans' complex Sm[N(SiMe$_3$)$_2$]$_2$(thf)$_2$ is currently being investigated as a powerful reductant for the solvent-dependent dehalogentation of alkyl halides.[43−45]

■ EXPERIMENTAL SECTION

General Considerations. All manipulations were performed under rigorous exclusion of air and moisture, using glovebox techniques (MB Braun MB200B; <1 ppm of O$_2$, <1 ppm of H$_2$O, argon atmosphere). The solvents *n*-hexane and tetrahydrofuran (thf) were purified using Grubbs columns (MBraun SPS, solvent purification system). 1,1,1,3,3,3-Hexamethyldisilazane HN(SiMe$_3$)$_2$ (95%), tellurium tetrabromide (99.999%), and hexachloroethane (99%) were purchased from Sigma-Aldrich and used as received, 1,2-diiodoethane (99%, Sigma-Aldrich) was recrystallized from diethyl ether prior to use, 1,2-dibromoethane (99% Sigma-Aldrich) was distilled and stored over freshly activated molecular sieve, ytterbium metal (99.9%, Sigma-Aldrich) and samarium and europium metal (both 99.9%, ABCR), and *n*-butyllithium (1.6 M in hexanes, Sigma-Aldrich) were used as received. Sodium bis(trimethylsilyl)amide was synthesized by reacting sodium amide (95%, Sigma-Aldrich) with 1.1 equiv of 1,1,1,3,3,3-hexamethyldisilazane in *n*-hexane. IR spectra were recorded on a Nicolet Protégé 460 instrument using DRIFT (diffuse reflectance infrared Fourier transform). For all of the DRIFT measurements, the ratio of potassium bromide to metal complex was kept constant at 20:1. Elemental analyses were performed on an Elementar Vario EL III apparatus. ^{1}H NMR spectra were recorded on Bruker Biospin DPX400 and Bruker AVII +400 instruments (^{1}H: 400.13 MHz) in C$_6$D$_6$ (99.6%, Sigma-Aldrich), which was degassed, dried over NaK alloy, filtered, and stored inside a glovebox or in [D$_8$]thf (99.5%, Euriso-top) which was distilled from NaK alloy and stored inside a glovebox. LnI$_2$(thf)$_2$ species (Ln = Sm, Eu, Yb, Tm) were synthesized according to published procedures.[41,42] Ln[N(SiMe$_3$)$_2$]$_2$(thf)$_2$ (Ln = Sm, Eu, Yb) were synthesized according to slightly modified literature procedures.[24]

[Sm{N(SiMe$_3$)$_2$}$_2$(μ-Cl)(thf)]$_2$ (1). Hexachloroethane (0.036 g, 0.15 mmol) was dissolved in thf (3 mL) and added dropwise to Sm[N(SiMe$_3$)$_2$]$_2$(thf)$_2$ (0.189 g, 0.31 mmol) dissolved in thf (5 mL). After the mixture was stirred for 5 min at ambient temperature, the solution turned from dark purple to pale yellow. The stirring was continued for another 18 h before the solvent was removed under vacuum, leaving a slightly sticky yellow solid (0.187 g). The solid was redissolved in a small amount of thf and crystallized at −40 °C. Crystallized yield (pale yellow): 0.044 g (0.04 mmol, 25%). ^{1}H NMR (400 MHz, [D$_8$]thf, 26 °C): δ 3.62 (m, 4H, thf O−C*H*$_2$), 1.77 (m, 4H, thf C*H*$_2$), −0.12 (s, 36H, Si(C*H*$_3$)$_3$) ppm. DRIFT (ν): 2950 (m), 2900 (w), 1462 (vw), 1412 (vw), 1286 (vw), 1259 (m), 1250 (s), 1018 (w), 947 (vs), 881 (m), 860 (s), 847 (vs), 827 (vs), 773 (m), 754 (m), 685 (m), 667 (s), 609 (m), 523 (vw), 417 (vw), 403 (vw) cm^{-1}. Anal. Calcd for C$_{32}$H$_{88}$Cl$_2$N$_4$O$_2$Si$_8$Sm$_2$ (1157.38 g/mol): C, 33.21; H, 7.66; N, 4.84. Found: C, 33.61; H, 7.77; N, 4.76.

[Sm{N(SiMe$_3$)$_2$}$_2$(μ-Br)(thf)]$_2$ (2). *Method a.* Tellurium tetrabromide (0.047 g, 0.11 mmol) was dissolved in thf (7 mL) and added dropwise to Sm[N(SiMe$_3$)$_2$]$_2$(thf)$_2$ (0.258 g, 0.42 mmol) dissolved in thf (3 mL). Shortly after addition a dark suspension formed. The mixture was stirred for 18 h and then centrifuged to remove elemental tellurium. The yellowish solution was filtered and the solvent removed under vacuum, leaving a dirty yellow solid (0.255 g). The solid was redissolved in a small amount of thf, filtered once more, and crystallized at −40 °C. Crystallized yield (colorless plates): 0.110 g (0.09 mmol, 43%).

Method b. 1,2-Dibromoethane (0.008 g, 0.04 mmol) was dissolved in thf (2 mL) and added dropwise to Sm[N(SiMe$_3$)$_2$]$_2$(thf)$_2$ (0.050 g, 0.08 mmol) dissolved in thf (1 mL). After the mixture was stirred for 5 min at ambient temperature, the solution turned from dark purple to pale yellow. The stirring was continued for another 18 h before the solvent was removed under vacuum, leaving an off-white to yellow solid in nearly quantitative yield. ^{1}H NMR (400 MHz, [D$_8$]thf, 26 °C): δ 3.62 (m, 4H, thf O−C*H*$_2$), 1.77 (m, 4H, thf C*H*$_2$), −0.19 (s, 36H, Si(C*H*$_3$)$_3$) ppm. DRIFT (ν): 2950 (m), 2900 (w), 1462−1286 multiple signals (vw), 1257 (m), 1244 (s), 1016 (w), 941 (vs), 879 (m), 849 (vs), 831 (vs), 773 (m), 766 (w), 669 (s), 611 (m), 526 (vw), 409 (vw) cm^{-1}. Anal. Calcd for C$_{32}$H$_{88}$Br$_2$N$_4$O$_2$Si$_8$Sm$_2$ (1248.31 g/mol): C, 30.84; H, 7.12; N, 4.50. Found: C, 30.91; H, 6.86; N, 4.50.

Sm[N(SiMe$_3$)$_2$]$_2$I(thf)$_2$ (3). Colorless crystals of 1,2-diiodoethane (0.051 g, 0.18 mmol) were dissolved in thf (5 mL) and added dropwise to Sm[N(SiMe$_3$)$_2$]$_2$(thf)$_2$ (0.223 g, 0.36 mmol) dissolved in thf (5 mL). During the addition, the solution turned from dark purple to light blue. After 30 min of stirring at ambient temperature, the solution finally turned pale yellow. The stirring was continued for another 18 h before the solvent was removed under vacuum, leaving a pale yellow solid (0.285 g). The solid was redissolved in a small amount of thf and crystallized at −40 °C. Crystallized yield (pale yellow): 0.154 g (0.23 mmol, 64%). ^{1}H NMR (400 MHz, [D$_8$]thf, 26 °C): δ 3.62 (m, 4H, thf O−C*H*$_2$), 1.77 (m, 4H, thf C*H*$_2$), −0.31 (s, 36H, Si(C*H*$_3$)$_3$) ppm. ^{1}H NMR (400 MHz, C$_6$D$_6$, 26 °C): δ 4.47 (s, br, 8H, thf O−C*H*$_2$), 1.65 (s, br, 8H, thf C*H*$_2$), −1.65 (s, 36H, Si(C*H*$_3$)$_3$) ppm. DRIFT (ν): 2950 (m), 2900 (w), 1464−1286 multiple signals (vw), 1248 (s), 1018 (w), 939 (vs), 877 (s), 845 (vs), 837 (vs), 771 (m), 687 (m), 669 (m), 611 (m), 523 (vw), 403 (w) cm^{-1}. Anal. Calcd for C$_{20}$H$_{54}$IN$_2$O$_2$Si$_4$Sm (743.25 g/mol): C, 32.36; H, 7.06; N, 3.77. Found: C, 28.73; H, 6.54; N, 4.09. Apparently, one molecule of thf was removed by applying vacuum. Anal. Calcd for C$_{16}$H$_{44}$IN$_2$OSi$_4$Sm (670.14 g/mol): C, 28.68; H, 6.62; N, 4.18. Found: C, 28.73; H, 6.54, N, 4.09.

Yb[N(SiMe$_3$)$_2$]$_2$Cl(thf)$_2$ (4). Hexachloroethane (0.083 g, 0.35 mmol) was dissolved in thf (4 mL) and added dropwise to Yb[N(SiMe$_3$)$_2$]$_2$(thf)$_2$ (0.448 g, 0.70 mmol) dissolved in thf (5 mL). Within 2 min of stirring at ambient temperature the solution turned from red to yellow. The stirring was continued for another 18 h before the solvent was removed under vacuum, leaving a yellow solid (0.469 g). The solid was redissolved in a small amount of thf and crystallized at −40 °C. Crystallized yield (three crystallization crops combined, yellow plates): 0.389 g (0.65 mmol, 93%). DRIFT (ν): 2954 (m), 2900 (w), 1462−1290 multiple bands (vw), 1261 (m), 1250 (s), 1041 (vw), 1012 (w), 941 (vs), 924 (vs), 885 (m), 850 (vs), 831 (vs), 779 (m), 756 (w), 700 (vw), 669 (m), 621 (w) cm^{-1}. Anal. Calcd for C$_{20}$H$_{52}$ClN$_2$O$_2$Si$_4$Yb (673.49 g/mol): C, 35.67; H, 7.78; N, 4.16. Found: C, 31.80; H, 7.83; N, 4.59. Apparently, one molecule of thf was removed by applying vacuum. Anal. Calcd for C$_{16}$H$_{44}$ClN$_2$OSi$_4$Yb (601.38 g/mol): C, 31.96; H, 7.37; N, 4.66. Found: C, 31.80; H, 7.83; N, 4.59.

Yb[N(SiMe$_3$)$_2$]$_2$Br(thf)$_2$ (5). Tellurium tetrabromide (0.039 g, 0.09 mmol) was added in small portions to a red solution of Yb[N(SiMe$_3$)$_2$]$_2$(thf)$_2$ (0.221 g, 0.35 mmol) in thf (5 mL). Shortly after addition, the clear red solution turned into a dark (black) suspension. The mixture was stirred for 18 h and then centrifuged to remove elemental tellurium. The dark yellow solution was filtered and the solvent removed under vacuum, leaving a brown-yellow solid (0.243 g). The solid was redissolved in a small amount of thf, filtered once more, and crystallized at −40 °C. Crystallized yield (yellow): 0.053 g (0.09 mmol, 26%). DRIFT (ν): 2951 (m), 2902 (w), 1460−1296 multiple signals (vw), 1248 (s), 1188 (vw), 1039 (vw), 1003 (w), 968 (vs), 949 (vs), 889 (m), 849 (vs), 833 (vs), 779 (m), 754 (w), 742 (vw), 696 (vw), 675 (m), 617 (w) cm^{-1}. Anal. Calcd for C$_{20}$H$_{52}$BrN$_2$O$_2$Si$_4$Yb (717.94 g/mol): C, 33.46; H, 7.30; N, 3.90. Found: C, 33.00; H, 7.38; N, 3.96.

Yb[N(SiMe$_3$)$_2$]$_2$I(thf)$_2$ (6). Colorless crystals of 1,2-diiodoethane (0.068 g, 0.24 mmol) were in thf (3 mL) and added dropwise to Yb[N(SiMe$_3$)$_2$]$_2$(thf)$_2$ (0.309 g, 0.48 mmol) dissolved in thf (4 mL). During the addition, the solution turned from red to orange and then dark yellow. After 18 h of stirring at ambient temperature, the solvent was removed under vacuum, leaving a dark yellow to orange solid (0.378 g). The solid was redissolved in a small amount of thf and crystallized at −40 °C. Crystallized yield: 0.230 g (0.33 mmol, 69%). DRIFT (ν): 2949 (m), 2902 (w), 1460−1298 multiple bands (vw), 1250 (s), 1043 (vw), 1001 (w), 966 (vs), 949 (vs), 887 (m), 849 (vs), 845 (vs), 779 (m), 756 (w), 742 (vw), 696 (vw), 675 (m), 619 (w) cm^{-1}. Anal. Calcd for C$_{20}$H$_{52}$IN$_2$O$_2$Si$_4$Yb (764.95 g/mol): C, 31.40; H, 6.85; N, 3.66. Found: C, 27.76; H, 6.31; N, 3.96. Apparently, one molecule of thf was removed by applying vacuum. Anal. Calcd for C$_{16}$H$_{44}$IN$_2$OSi$_4$Yb (692.84 g/mol): C, 27.74; H, 6.40; N, 4.04. Found: C, 27.76; H, 6.31; N, 3.96.

[Eu{N(SiMe$_3$)$_2$}$_3$Cl][(thf)$_5$Eu(μ-Cl)$_2$Eu(thf)$_5$] (7). Hexachloroethane (0.038 g, 0.16 mmol) was dissolved in thf (3 mL) and added dropwise to a solution of Eu[N(SiMe$_3$)$_2$]$_2$(thf)$_2$ (0.198 g, 0.32 mmol) in thf (3 mL). After 4 h the solution had turned from yellow to dark yellow. The reaction mixture was stirred for 18 h before the solvent was removed under vacuum, leaving an orange-red solid (0.192 g). The solid was redissolved in a small amount of thf and stored at −40 °C, forming shapeless orange crystals, which were identified by X-ray crystallography as [Eu{N(SiMe$_3$)$_2$}$_3$Cl][(thf)$_5$Eu(μ-Cl)$_2$Eu(thf)$_5$], 0.134 g (0.08 mmol, 72% on Eu). DRIFT (ν): 2953 (m), 2899 (w), 1448 (vw), 1410 (vw), 1248 (s), 1178 (shoulder, vw), 1038 (shoulder vw), 985 (vs), 949 (shoulder, w), 860 (s), 831 (vs), 768 (m), 677 (w), 660 (w), 604 (m) cm^{-1}. Anal. Calcd for C$_{58}$H$_{134}$Cl$_3$Eu$_3$N$_3$O$_{10}$Si$_6$ (1764.47 g/mol): C, 39.48; H, 7.66; N, 2.38. Found: C, 29.71; H, 6.59; N, 4.36. Better analysis could not be obtained, most likely due to incomplete combustion.

[Eu{N(SiMe$_3$)$_2$}$_2$(μ-Cl)(thf)]$_2$ (8). A colorless thf solution (4 mL) of trityl chloride (0.139 g, 0.50 mmol) was added dropwise to a yellow solution of Eu[N(SiMe$_3$)$_2$]$_2$(thf)$_2$ (0.307 g, 0.50 mmol) in thf (3 mL). During the addition, the solution turned from yellow to orange and then red. The reaction mixture was stirred for 1 h before the solvent was reduced under vacuum, leaving a red oil, which was stored at −40 °C. After 24 h shapeless orange crystals of **8** appeared, accompanied by colorless prisms of Gomberg's dimer, the trityl radical coupling product. This contamination hampered yield determination and further analyses.

[Tm{N(SiMe$_3$)$_2$}$_2$(μ-Cl)(thf)]$_2$ (9). In a 15 mL pressure tube, Tm filings (0.119 g, 0.70 mmol) were reacted with I$_2$ (0.150 g, 0.59 mmol) in thf (6 mL) for 2 h at 75 °C. The mixture was centrifuged and filtered, resulting in an emerald green solution, which was cooled to −40 °C. Na[N(SiMe$_3$)$_2$] (0.206 g, 1.12 mmol) dissolved in chilled thf (−40 °C, 4 mL) was added slowly, and the reaction mixture was stirred for 30 min at −40 °C. Hexachloroethane (0.066 g, 0.28 mmol) dissolved in cold thf (2 mL) was slowly added to the reaction mixture, which turned from dark brown-green to pale amber. The mixture was warmed to ambient temperature within 30 min. Then the solvent was removed under vacuum, the solid residue was extracted three times with *n*-hexane, centrifuged, and filtered, and the pale amber solution was dried under vacuum, leaving an off-white solid (0.278 g). The solid was dissolved in a small amount of *n*-hexane, filtered once more, and then crystallized at −40 °C, yielding colorless rhombohedrons of compound **9**. Determination of the yield was hampered due to cocrystallization of Tm[N(SiMe$_3$)$_2$]$_3$. Crystals of **9** were manually separated from the colorless needles of Tm[N(SiMe$_3$)$_2$]$_3$ under a light microscope. Anal. Calcd for C$_{32}$H$_{88}$Cl$_2$N$_4$O$_2$Si$_8$Tm$_2$ (1194.54 g/mol): C, 32.18; H, 7.43; N, 4.69. Found: C, 31.51; H, 7.10; N, 4.47. Unfortunately, the manually purified amounts of compound **9** were only sufficient to perform an elemental analysis, but not DRIFT.

Tm[N(SiMe$_3$)$_2$]I$_2$(thf)$_3$·(thf) (10). In a 15 mL pressure tube, Tm filings (0.127 g, 0.75 mmol) were reacted with I$_2$ (0.151 g, 0.59 mmol) in 5 mL of thf for 2 h at 75 °C. The mixture was centrifuged and filtered, resulting in an emerald green solution, which was cooled to −40 °C. Further thf was added to give a total volume of 7 mL. K[N(SiMe$_3$)$_2$] (0.225 g, 1.13 mmol) was slowly added in portions, and the reaction mixture was stirred for 30 min at −40 °C. Colorless crystals of 1,2-diiodoethane (0.083 g, 0.30 mmol) dissolved in 2 mL of cold thf were slowly added to the reaction mixture, which turned from dark brown-green to pale amber. The mixture was warmed to ambient temperature and was stirred for an additional 18 h. The reaction mixture was centrifuged and the amber solution separated from off-white solids and filtered. Drying under vacuum left a pale yellow solid (0.475 g). The solid was dissolved in a small amount of thf, filtered once more, and then crystallized at −40 °C, yielding a few single crystals of compound **10**, sufficient for an X-ray structure analysis.

■ ASSOCIATED CONTENT

Ⓢ Supporting Information

The Supporting Information is available free of charge on the ACS Publications website at DOI: 10.1021/acs.inorgchem.8b00240.

^{1}H NMR spectra of samarium complexes **1**−**3** and experimental description of X-ray structure analyses and associated crystallographic data for all structures, including figures and selected geometric parameters, for structures **1**,

2, **8**, **9**, $Eu[N(SiMe_3)_2]_2(thf)_2$, $Yb[N(SiMe_3)_2]_2(thf)_2$, and $Tm[N(SiMe_3)_2]_3$ (PDF)

Accession Codes

CCDC 1814971−1814983 contain the supplementary crystallographic data for this paper. These data can be obtained free of charge via www.ccdc.cam.ac.uk/data_request/cif, or by emailing data_request@ccdc.cam.ac.uk, or by contacting The Cambridge Crystallographic Data Centre, 12 Union Road, Cambridge CB2 1EZ, UK; fax: +44 1223 336033.

■ AUTHOR INFORMATION

Corresponding Author

*R.A.: fax, (+49) 07071/29 2436; e-mail, reiner.anwander@uni-tuebingen.de.

ORCID

Karl W. Törnroos: 0000-0001-6140-5915
Reiner Anwander: 0000-0002-1543-3787

Notes

The authors declare no competing financial interest.

■ ACKNOWLEDGMENTS

We thank the Norwegian Research Council (Project No. 182547/I30) and the L. Meltzer Høyskolefond (Bursary No. 2017/3273).

■ REFERENCES

(1) For review articles, see: (a) Bradley, D. C.; Chisholm, M. H. Transition-Metal Dialkylamides and Disilylamides. *Acc. Chem. Res.* **1976**, *9*, 273−280. (b) Harris, D. H; Lappert, M. F. In *Organometallic Chemistry Reviews: Organosilicon Reviews*; Elsevier Scientific: Amsterdam, 1976; pp 13−102. (c) *Metal and Metalloid Amides*; Lappert, M. F., Power, P. P., Sanger, A. R., Srivastava, R. C., Eds.; Ellis Horwood: Chichester, U.K., 1980. (d) Anwander, R. Lanthanide Amides. *Top. Curr. Chem.* **1996**, *179*, 33−112. (e) Kempe, R. Highlights in the Renaissance of Amidometal Chemistry. *Angew. Chem., Int. Ed.* **2000**, *39*, 468−493. (f) Piers, W. E.; Emslie, D. J. H. Non-cyclopentadienyl ancillaries in organogroup 3 metal chemistry: a fine balance in ligand design. *Coord. Chem. Rev.* **2002**, *233−234*, 131−155. (g) *Metal Amide Chemistry*; Lappert, M. F., Protchenko, A. V., Power, P. P., Seeber, A. L., Eds.; Wiley: Hoboken, NJ, 2009. (h) Liang, Y.; Anwander, R. Nanostructured catalysts via silylamide-based smart grafting. *Dalton Trans.* **2013**, *42*, 12521−12545.

(2) (a) Meermann, C.; Sirsch, P.; Törnroos, K. W.; Anwander, R. Synthesis and structural characterization of scandium SALEN complexes. *Dalton Trans.* **2006**, 1041−1050. (b) Xu, X.; Zhang, Z.; Yao, Y.; Zhang, Y.; Shen, Q. Controlled Synthesis, Characterization, and Reactivity of Neutral and Anionic Lanthanide Amides Supported by Methylene-Linked Bis(phenolate) Ligands. *Inorg. Chem.* **2007**, *46*, 9379−9388. (c) Sun, S.; Sun, Q.; Zhao, B.; Zhang, Y.; Shen, Q.; Yao, Y. Unexpected C−H Bond Activation Promoted by Bimetallic Lanthanide Amido Complexes Bearing a META-Phenylene-Bridged Bis(β-diketiminate) Ligand. *Organometallics* **2013**, *32*, 1876−1881.

(3) Li, H.-X.; Xu, Q.-F.; Chen, J.-X.; Cheng, M.-L.; Zhang, Y.; Zhang, W.-H.; Lang, J.-P.; Shen, Q. Syntheses, crystal structures and catalytic properties of a series of lanthanide(III) bis(trimethylsilyl)amide chloride complexes: $[\{((Me_3Si)_2N)_2Nd(\mu'\text{-}Cl)Li(THF)_3\}(\mu\text{-}Cl)]_2$, $[\{((Me_3Si)_2N)_2Ln(\mu'\text{-}Cl)Li(THF)_2\}(\mu_3\text{-}Cl)]_2$ (Ln = Eu, Ho), and $[\{(Me_3Si)_2NLn(\mu'\text{-}Cl)_2Li(THF)_2\}(\mu\text{-}Cl)]_2$ (Ln = Nd, Sm, Eu, Ho, Yb). *J. Organomet. Chem.* **2004**, *689*, 3438−3448.

(4) Bradley, D. C.; Ghotra, J. S.; Hart, F. A. 3-Coordination in Lanthanide Chemistry - Tris[Bis(Trimethylsilyl)Amido] Lanthanide(III) Compounds. *J. Chem. Soc., Chem. Commun.* **1972**, *6*, 349−350.

(5) Tilley, T. D.; Zalkin, A.; Andersen, R. A.; Templeton, D. H. Divalent Lanthanide Chemistry - Preparation of Some 4-Coordinate and 6-Coordinate Bis[(Trimethylsilyl)amido] Complexes of Europium(II) - Crystal-Structure of Bis[Bis(Trimethylsilyl)amido]Bis(1,2-Dimethoxyethane)europium(II). *Inorg. Chem.* **1981**, *20*, 551−554.

(6) Aspinall, H. C.; Bradley, D. C.; Hursthouse, M. B.; Sales, K. D.; Walker, N. P. C.; Hussain, B. Preparation of the bis(trimethylsilyl)amido lanthanide chlorides $[\{Ln[N(SiMe_3)_2]_2(\mu\text{-}Cl)(thf)\}_2]$ (thf = tetrahydrofuran), and the crystal and molecular structures of the gadolinium and ytterbium complexes. *J. Chem. Soc., Dalton Trans.* **1989**, *4*, 623−626.

(7) Berg, D. J.; Gendron, R. A. Synthesis, solid state structure, and solution behaviour of the lighter lanthanide bis(trimethylsilyl)amido chlorides, $[Ln\{N(SiMe_3)_2\}_2(THF)(\mu\text{-}Cl)]_2$ (Ln = Ce, Nd). *Can. J. Chem.* **2000**, *78*, 454−458.

(8) Karl, M.; Seybert, G.; Massa, W.; Agarwal, S.; Greiner, A.; Dehnicke, K. Kristallstrukturen der Samarium-Amido-Komplexe $[Sm(I\text{-}X)\{N(SiMe_3)_2\}_2(THF)]_2$ mit X = Cl, Br. *Z. Anorg. Allg. Chem.* **1999**, *625*, 1405−1407.

(9) Trifonov, A.; Lyubov, D.; Fedorova, E.; Skvortsov, G.; Fukin, G.; Kurskii, Y.; Bochkarev, M. Mixed-ligand guanidinate derivatives of rare-earth metals. Molecular structures of $\{(Me_3Si)_2NC(N\text{-}cyclo\text{-}Hex)_2\}Y[N(SiMe_3)_2]_2$, $[\{(Me_3Si)_2NC(N\text{-}cyclo\text{-}Hex)_2\}YbI(THF)_2]_2$, and $[\{(Me_3Si)_2N\}_2Y(THF)(\mu\text{-}Cl)]_2$ complexes. *Russ. Chem. Bull.* **2006**, *55*, 435−441.

(10) Zhou, F.; Zhang, S.; Zhao, Y.; Zhang, C.; Cheng, X.; Zheng, L.; Zhang, Y.; Li, Y. Z. Dinuclear Dysprosium and Ytterbium Complexes Incorporating N,N-Bis(pyrrolyl-α-methyl)-N-methylamine Ligand: Syntheses and Structures. *Z. Anorg. Allg. Chem.* **2009**, *635*, 2636−2641.

(11) Hemmer, E.; Cavelius, C.; Huch, V.; Mathur, S. Templating Influence of Molecular Precursors on $Pr(OH)_3$ Nanostructures. *Inorg. Chem.* **2015**, *54*, 6267−6280.

(12) Collin, J.; Giuseppone, N.; Jaber, N.; Domingos, A.; Maria, L.; Santos, I. Iodo bis bistrimethylsilylamido lanthanides. *J. Organomet. Chem.* **2001**, *628*, 271−274.

(13) Schumann, H.; Winterfeld, J.; Rosenthal, E. C. E.; Hemling, H.; Esser, L. Metallorganische Verbindungen der Lanthanoide. 88. Monomere Lanthanoid(III)-amide: Synthese und Röntgenstrukturanalyse von $[Nd\{N(C_6H_5)(SiMe_3)\}_3(THF)]$, $[Li(THF)_2(\mu\text{-}Cl)_2Nd\{N(C_6H_3Me_2\text{-}2,6)(SiMe_3)\}_2(THF)]$ und $[ClNd\{N(C_6H_3\text{-}iso\text{-}Pr_2\text{-}2,6)(SiMe_3)\}_2(THF)]$. *Z. Anorg. Allg. Chem.* **1995**, *621*, 122−130.

(14) Hitchcock, P. B.; Huang, Q.-G.; Lappert, M. F.; Wei, X.-H. Lanthanide metal amides revisited; the use of the 2,2,6,6-tetramethylpiperidinato (TMP) ligand. *J. Mater. Chem.* **2004**, *14*, 3266−3273.

(15) Spallek, T.; Heß, O.; Meermann-Zimmermann, M.; Meermann, C.; Klimpel, M. G.; Estler, F.; Schneider, D.; Scherer, W.; Tafipolsky, M.; Törnroos, K. W.; Maichle-Mössmer, C.; Sirsch, P.; Anwander, R. Synthesis and structural diversity of rare-earth metal di*iso*propylamide complexes. *Dalton Trans.* **2016**, *45*, 13750−13765.

(16) Niemeyer, M. Synthesis and Structural Characterization of Several Ytterbium Bis(trimethylsilyl)amides Including Base-free $[Yb\{N(SiMe_3)_2\}_2(\mu\text{-}Cl)]_2$ − A Coordinatively Unsaturated Complex with Additional Agostic $Yb\cdots(H_3C{-}Si)$ Interactions. *Z. Anorg. Allg. Chem.* **2002**, *628*, 647−657.

(17) Meermann, C.; Törnroos, K. W.; Nerdal, W.; Anwander, R. Rare-Earth Metal Mixed Chloro/Methyl Compounds: Heterogeneous−Homogeneous Borderline Catalysts in 1,3-Diene Polymerization. *Angew. Chem., Int. Ed.* **2007**, *46*, 6508−6513.

(18) Zhou, L.; Wang, J.; Zhang, Y.; Yao, Y.; Shen, Q. Synthesis and Structural Characterization of a Series of Lanthanide(II) Amides: Steric Effect of Amido Ligand. *Inorg. Chem.* **2007**, *46*, 5763−5772.

(19) Minhas, R. K.; Ma, Y.; Song, J. I.; Gambarotta, S. Synthesis, Reactivity, and Stability of Di- and Trivalent Samarium Amides. *Inorg. Chem.* **1996**, *35*, 1866.

(20) Crozier, A. R.; Bienfait, A. M.; Maichle-Mössmer, C.; Törnroos, K. W.; Anwander, R. A homoleptic tetravalent cerium silylamide. *Chem. Commun.* **2013**, *49*, 87−89.

(21) Karl, M.; Seybert, G.; Massa, W.; Dehnicke, K. $[ScCl_2\{N(SiMe_3)_2\}(THF)_2]$ als Vorläufer für die Synthese von Scandiumnitrid. *Z. Anorg. Allg. Chem.* **1999**, *625*, 375−376.

(22) Hitchcock, P. B.; Hulkes, A. G.; Lappert, M. F. Oxidation in Nonclassical Organolanthanide Chemistry: Synthesis, Characterization,

and X-ray Crystal Structures of Cerium(III) and -(IV) Amides. *Inorg. Chem.* **2004**, *43*, 1031−1038.

(23) Schädle, C.; Meermann, C.; Törnroos, K. W.; Anwander, R. Rare-Earth Metal Phenyl(trimethylsilyl)amide Complexes. *Eur. J. Inorg. Chem.* **2010**, 2841−2852.

(24) Evans, W. J.; Drummond, D. K.; Zhang, H. M.; Atwood, J. L. Synthesis and X-ray crystal structure of the divalent [bis(trimethylsilyl)-amido] samarium complexes $[(Me_3Si)_2N]_2Sm(THF)_2$ and $\{[(Me_3Si)_2N]Sm(\mu\text{-}I)(DME)(THF)\}_2$. *Inorg. Chem.* **1988**, *27*, 575−579.

(25) Tilley, T. D.; Anderson, R. A.; Zalkin, A. Tertiary phosphine complexes of the f-block metals. Crystal structure of $Yb[N(SiMe_3)_2]_2[Me_2PCH_2CH_2PMe_2]$: evidence for a ytterbium-γ-carbon interaction. *J. Am. Chem. Soc.* **1982**, *104*, 3725−3727.

(26) (a) Deacon, G. B.; Forsyth, C. M.; Wilkinson, D. L. Diverse Heteroleptic ytterbium(III) thiocyanate complexes by oxidation from bis(thiocyanato)ytterbium(II). *Chem. - Eur. J.* **2001**, *7*, 1784−1795. (b) Deacon, G. B.; Meyer, G.; Stellfeldt, D.; Zelesny, G.; Skelton, B. W.; White, A. H. Syntheses of Bis(aryloxo)halogenoytterbium(III) Complexes: $[Yb(OAr)_2X(THF)_2]$ (X = Cl, Br, I; OAr = OC_6H_2−2,6-tBu$_2$−4-R; R = H, Me, tBu) and the X-Ray Crystal Structures of $[Yb(OC_6H_2\text{−}2,6\text{-}t\text{Bu}_2\text{-}4\text{-}Me)_2I(THF)_2]$ and $[Yb(OC_6H_3\text{-}2,6\text{-}t\text{Bu}_2)_2OH(THF)]_2$. *Z. Anorg. Allg. Chem.* **2001**, *627*, 1652−1658.

(27) Hou, Z.; Fujita, A.; Yoshimura, T.; Jesorka, A.; Zhang, Y.; Yamazaki, H.; Wakatsuki, Y. Heteroleptic Lanthanide Complexes with Aryloxide Ligands. Synthesis and Structural Characterization of Divalent and Trivalent Samarium Aryloxide/Halide and Aryloxide/Cyclopentadienide Complexes. *Inorg. Chem.* **1996**, *35*, 7190−7195.

(28) Williams, U. J.; Carroll, P. J.; Schelter, E. J. Synthesis and Analysis of a Family of Cerium(IV) Halide and Pseudohalide Compounds. *Inorg. Chem.* **2014**, *53*, 6338−6345.

(29) Evans, W. J.; Grate, J. W.; Levan, K. R.; Bloom, I.; Peterson, T. T.; Doedens, R. J.; Zhang, H.; Atwood, J. L. Synthesis and X-ray crystal structure of di(pentamethylcyclopentadienyl)lanthanide and yttrium halide complexes. *Inorg. Chem.* **1986**, *25*, 3614−3619.

(30) Arnold, P. L.; Turner, Z. R.; Kaltsoyannis, N.; Pelekanaki, P.; Bellabarba, R. M.; Tooze, R. P. Covalency in Ce^{IV} and U^{IV} Halide and N-Heterocyclic Carbene Bonds. *Chem. - Eur. J.* **2010**, *16*, 9623−9629.

(31) Agarwal, S.; Karl, M.; Dehnicke, K.; Seybert, G.; Massa, W.; Greiner, A. Ring-opening polymerization of ε-caprolactone and δ-valerolactone using new Sm(III) μ-halo-bis(trimethylsilyl)amido complexes. *J. Appl. Polym. Sci.* **1999**, *73*, 1669−1674.

(32) Rabe, G. W.; Yap, G. P. A. Crystal structure of samarium tris[bis(dimethylsilyl)amide]bis(tetrahydrofuran), $Sm[N(SiHMe_2)_2]_3(THF)_2$. *Z. Kristallogr. - New Cryst. Struct.* **2000**, *215*, 457−458.

(33) Yao, Y.-M.; Shen, Q.; Zhang, Y.; Xue, M.-Q.; Sun, J. Syntheses and reactivities of bisaryloxo lanthanide chlorides and crystal structures of $[Ln(ArO)_2Cl(THF)_2]\cdot(MePh)$ (Ln = Er, Yb) and $[Sm(ArO)_2(THF)_3]\cdot(MePh)$ (ArO= 2,6-di-*tert*-butyl-4-methylphenoxo). *Polyhedron* **2001**, *20*, 3201−3208.

(34) Bienfait, A. M.; Wolf, B. M.; Törnroos, K. W.; Anwander, R. Ln(II)/Pb(II)−Ln(III)/Pb(0) Redox Approach toward Rare-Earth-Metal Half-Sandwich Complexes. *Organometallics* **2015**, *34*, 5734−5744.

(35) Martín-Vaca, B.; Dumitrescu, A.; Gornitzka, H.; Bourissou, D.; Bertrand, G. Synthesis and structural characterization of unusual amido samarium(III) complexes. *J. Organomet. Chem.* **2003**, *682*, 263−266.

(36) Westerhausen, M.; Hartmann, M.; Pfitzner, A.; Schwarz, W. Bis(trimethylsilyl)amide und -methanide des Yttriums - Molekülstrukturen von Tris(diethylether-O)lithium-(μ-chloro)-tris[bis(trimethylsilyl) methyl]yttriat, solvensfreiem Yttrium-tris[bis(trimethylsilyl)amid] sowie dem Bis(benzonitril)-Komplex. *Z. Anorg. Allg. Chem.* **1995**, *621*, 837.

(37) Eisenstein, O.; Hitchcock, P. B.; Hulkes, A. G.; Lappert, M. F.; Maron, L. Cerium masquerading as a Group 4 element: synthesis, structure and computational characterisation of $[CeCl\{N(SiMe_3)_2\}_3]$. *Chem. Commun.* **2001**, 1560−1561.

(38) Bochkarev, L. N.; Molosnova, N. E.; Zakharov, L. N.; Fukin, G. K.; Yanovsky, A. I.; Struckhov, Y. T. Synthesis and structure of triphenylmethyl derivatives of ytterbium $[Yb(THF)_6]^{2+}[Ph_3C]_2^-$ and $[(THF)_4Yb(\mu\text{-}Cl)_2Yb(THF)_4]^{2+}$ $[Ph_3Cl]_2^-$. *J. Organomet. Chem.* **1995**, *485*, 101−107.

(39) Heckmann, G.; Niemeyer, M. Synthesis and First Structural Characterization of Lanthanide(II) Aryls: Observation of a Schlenk Equilibrium in Europium(II) and Ytterbium(II) Chemistry. *J. Am. Chem. Soc.* **2000**, *122*, 4227−4228.

(40) Evans, W. J.; Zucchi, G.; Ziller, J. W. Dinitrogen Reduction by Tm(II), Dy(II), and Nd(II) with Simple Amide and Aryloxide Ligands. *J. Am. Chem. Soc.* **2003**, *125*, 10−11.

(41) Namy, J. L.; Girard, P.; Kagan, H. B. A new preparation of some divalent lanthanide iodides and their usefulness in organic synthesis. *Nouv. J. Chim.* **1977**, *1*, 5.

(42) Bochkarev, M. N.; Fedushkin, I. L.; Fagin, A. A.; Petrovskaya, T. V.; Ziller, J. W.; Broomhall-Dillard, R. N. R.; Evans, W. J. Synthesis and Structure of the First Molecular Thulium(II) Complex: $[TmI_2(MeOCH_2CH_2OMe)_3]$. *Angew. Chem., Int. Ed. Engl.* **1997**, *36*, 133.

(43) Szostak, M.; Procter, D. J. Beyond Samarium Diiodide: Vistas in Reductive Chemistry Mediated by Lanthanides. *Angew. Chem., Int. Ed.* **2012**, *51*, 9238−9256.

(44) (a) Prasad, E.; Knettle, B. W.; Flowers, R. A., II Investigation of the $[Sm\{N(SiMe_3)_2\}_2(thf)_2]$ Reducing System in THF. Rate and Mechanistic Studies. *J. Am. Chem. Soc.* **2002**, *124*, 14663−14667. (b) Chciuk, T. V.; Maity, S.; Flowers, R. A., II Kinetic solvent effects in the reduction of alkyl halides by $Sm[N(SiMe_3)_2]_2(thf)_2$. *J. Organomet. Chem.* **2018**, *857*, 52−57 and references therein.

(45) (a) Janjetovic, M.; Traff, A. M.; Ankner, T.; Wettergren, J.; Hilmersson, G. Solvent dependent reductive defluorination of aliphatic C−F bonds employing $Sm(HMDS)_2$. *Chem. Commun.* **2013**, *49*, 1826−1828. (b) Chciuk, T. V.; Hilmersson, G.; Flowers, R. A., II Solvent-Dependent Substrate Reduction by $\{Sm[N(SiMe_3)_2]_2(thf)_2\}$. An Alternative Approach for Accelerating the Rate of Substrate Reduction by Sm(II). *J. Org. Chem.* **2014**, *79*, 9441−9443.

DOI: 10.1021/acs.inorgchem.8b00240